Geophysical Research Letters

Supporting Information for

Factors controlling the evaporation of secondary organic aerosol from α-pinene ozonolysis

Taina Yli-Juuti[1], Aki Pajunoja[1], Olli-Pekka Tikkanen[1], Angela Buchholz[1], Celia Faiola[1], Olli Väisänen[1], Liqing Hao[1], Eetu Kari[1], Otso Peräkylä[2], Olga Garmash[2], Manabu Shiraiwa[3], Mikael Ehn[2], Kari Lehtinen[1] and Annele Virtanen[1]

[1]Department of Applied Physics, University of Eastern Finland, P.O. Box 1627, 70211 Kuopio, Finland.

[2]Department of Physics, University of Helsinki, P.O. Box 64, 00014 Helsinki, Finland.

[3]Department of Chemistry, University of California Irvine, 92697-2025 Irvine, CA, USA.

[4]Finnish Meteorological Institute, P.O. Box 1627, 70211, Kuopio, Finland.

Contents of this file

Additional Supporting Information (Files uploaded separately)

Introduction

Supporting information includes additional explanation of the experimental system, description of the models, supplementary figures and a movie of a model simulation.

Text S1.

1 Experimental methods

Experiments were performed at the University of Eastern Finland (Kuopio) in the aerosol laboratory of the Department of Applied Physics. Both gas phase and particle phase were monitored with a comprehensive suite of instrumentation including a Scanning Mobility Particle Sizer (SMPS), Aerosol Mass Spectrometer (AMS) and 2 CPCs for monitoring the particle phase, and Proton Transfer Reaction Time of Flight Mass Spectrometer (PTR-ToF-MS), O_3-monitor and RH-probes for monitoring the gas phase. The basic experimental setup is presented in Fig. S1.

1.1 Glass flow tube – Particle generation

SOA was generated via α-pinene ozonolysis in a continuous flow reactor made of quartz (4.5 m length, 0.056 m diameter). The α-pinene (Sigma-Aldrich, 98%) was introduced to the flow reactor by flowing 0.13 lpm of clean air through a diffusion source, which was constructed from a glass bottle with a vial of α-pinene inside. VOC flow was controlled with a needle valve. Ozone was generated via photodissociation of oxygen in 0.6 lpm of clean air with a stable ozone generator (UVP, part # 97-0067-02). Dilution air was added at the inlet of the flow tube to adjust particle mass loadings and particle size. Dilution flow ranged from 1-6 lpm. A vacuum flow was also added upstream of the flow reactor to enable additional dilution of the α-pinene/ozone mixture while maintaining the low flow rates through the flow reactor that were needed to grow the particles. Vacuum flows ranged from 0-3.5 lpm. Total flow through the flow reactor 2.5-3.33 lpm (average residence times in the flow tube ranged from 3.3-4.4 min). All flows were controlled with mass flow controllers unless otherwise noted. The polydisperse mass loadings in the flow reactor was 100-130 μg m^{-3}. High polydisperse mass loadings had to be used to ensure there was enough monodisperse particle mass to conduct the evaporation experiments. Geometric mean diameter was 51±2 nm. SOA was generated under dry condition in all experiments except was one dry evaporation experiment (experiment 1) where particles were formed at 30% RH.

1.2 DMA – Particle sampling and size selection

The first Differential Mobility Analyzer (DMA1) selected a nearly monodisperse particle population from the generated SOA population. The selected particle size was 80 nm. A nano-DMA (TSI, model 3085) or a short Vienna style DMA (custom made) was used with open loop sheath flow configuration using sheath flow of 8.5 or 10 lpm and sample flow of 0.3 or 1.5 lpm, respectively, depending on the desired residence time. The total flow in DMA1 leads to a drifting time of 0.2-0.3 s (nano-DMA) or 0.8-0.9 s (Vienna-DMA) inside DMA1 [*Li and Chen*, 2005]. The nano-DMA was used in dry experiment 1 and the short Vienna style DMA was used in all other experiments. Ozone was removed by passing the SOA through an ozone scrubber (copper tubing coated with dried KI solution) before entering DMA1 to prevent oxidation reactions in the evaporation chamber. Purified air was used for the sheath air and therefore the gas phase of the sample at the exit from the DMA1 can be assumed to be clean air. This was confirmed by PTR-ToF-MS and O_3-monitor measurements. In case of 40% and 80% RH experiments the sheath air of DMA1 was humidified with a Nafion humidifier. The RH was measured with Vaisala sensors (HMP 110) just before the inlet and after the outlet of the evaporation chamber. RH in the evaporation chamber was 39±0.5% (40% RH) and 78±1% (80% RH).

1.3 Evaporation chamber – Varying evaporation time

After DMA1 the nearly monodisperse particle population was fed into the evaporation chamber. The evaporation chamber is a 100 L (length 1.5 m) cylindrical stainless steel chamber with an inlet in the center of the upper end of the chamber and an outlet at center of the lower end. To prevent turbulence in the flow, laminar nets were installed at the top and bottom of the chamber. Particles were supplied continuously to the chamber until the desired concentration in the chamber was reached. After this the voltage in DMA1 was set to zero to provide air with the same gas phase composition but without particles. This was necessary to replenish the sampled volume in the chamber. After filling, the instruments were disconnected and the chamber closed. Sampling was resumed for approx. 20 min at a time to collect data points for long residence times. Gas phase composition, particle size and composition were monitored during filling of the chamber providing data points with 20-30 min residence time. Shorter residence time data points (2.5-130 s) were achieved by increasing the tube length between the DMA1 and SMPS (i.e. bypassing mode shown in the Fig. S1).

1.3.1 SMPS – Measuring the size of the evaporated particles

Particle size distribution was measured with a Scanning Mobility Particle Sizer (SMPS, TSI model 3080 platform accompanied with CPC TSI model 3775 or 3772). The DMA1 and SMPS systems were calibrated with ammonium sulfate (AS) particles at dry conditions before and after the campaign with multiple particle sizes. The TSI 3080 platform uses closed loop sheath flow configuration. The flow circulation unit consist of HEPA filters and an air circulation pump. For the filling of the evaporation chamber high sample flows were used in the SMPS to reduce filling time (3775 high flow mode, 1.5 lpm, or 3772, 1.0 lpm). The later sampling from the evaporation chamber was done with sample flows of 0.3 lpm (3775, low flow mode) or 1.0 lpm (3772). For short residence time measurements in bypassing mode, low flows were used in the SMPS. For the RH40% and RH80% experiments the SMPS was continuously sampling from air at the target RH, thus ensuring that the RH in the closed loop stayed close to that in the evaporation chamber.

1.3.2 HR-ToF-AMS – Measuring the chemical composition of the particles

Particle chemical composition was measured with an Aerodyne High-resolution Time-of-flight Aerosol Mass Spectrometer (AMS, Aerodyne). Detailed description of the instrument, measurement and data processing are presented elsewhere [*DeCarlo et al.*, 2006]. Briefly, AMS measures the non-refractory composition of sub-micrometer aerosols before and after the evaporation chamber. The V-mode mass spectra were analyzed using standard TOF-AMS data analysis toolkits (SQUIRREL 1.56A and PIKA 1.15). A particle collection efficiency factor of 0.5 was applied to account for the loss of particles in the aerodynamic transmission lens and vaporizer. The relatively ionization efficiency values of 1.1, 1.2, 1.3, 1.4 and 3.7 were used for nitrate, sulfate, chloride, organic and ammonium, respectively. An elemental analysis was processed to determine the ratio of oxygen to carbon atoms (O:C) taking into account CHO^+ ion correction [Aiken et al., 2007; Canagaratna et al., 2015]. The particle mass in the monodisperse particle population evaporation experiments was too low for AMS experiments. Therefore, a separate evaporation experiment was performed for particle composition measurements. In this experiment, the polydisperse particle population was diluted after the O_3 scrubber with 10 lpm of clean air at the desired RH and led directly to the evaporation chamber, i.e. DMA1 was bypassed. The clean air was added to reduce the gas phase concentrations of organics and to set the desired RH.

1.3.3 PTR-ToF-MS – Measuring the gas phase composition

A proton-transfer-reaction time-of-flight mass spectrometer (PTR-ToF-MS, PTR-TOF 8000 Ionicon Analytik, Austria) was used to measure the gas-phase compounds during the experiments. The PTR-ToF-MS measured from two points in the setup: after DMA1, and after the evaporation chamber. After DMA1, the gas-phase was measured in order to verify the DMA's effect of dilution on the gas phase compounds. After the evaporation chamber, the PTR-ToF-MS was used to monitor the gas-phase compounds formed due to evaporation. The PTR-TOF was operated under the following conditions: drift tube voltage and temperature were set to 600 V and 60 ˚C respectively, drift pressure 2.30 mbar, and E/N was set to 130 Td. The sampling rate of the PTR-TOF was 160 ml min^{-1} through heated PEEK (I.D. 1 mm) tubing (temperature 60 ˚C) to minimize wall losses in the sampling line.

2 Modelling

The evaporation was simulated using two models. One of the models simulates the evaporation of a well-mixed liquid-like particle and the other model can simulate the evaporation of semi-solid particles since the particle phase is represented with a layered structure.

2.1 Well-mixed particle evaporation model

The "traditional" well-mixed particle evaporation model assumes liquid-like particles for which particle phase molecular transport kinetics do not limit the evaporation, i.e. the particle phase mixing time scale is shorter that the time scale of evaporation. The composition and size evolution of the particles and the evolution gas phase concentrations are obtained by solving the differential equations for the number of organic molecules in a particle and in the gas phase [*Vesala et al.*, 1997; *Lehtinen and Kulmala*, 2003]

$$\frac{dN_{p,i}}{dt} = \frac{2\pi\left(d_i + d_p\right)\left(D_{air,i} + D_{air,p}\right)\beta_i}{k_B T}\left(p_{\infty,i} - p_{eq,i}\right) \quad \text{(S1)}$$

$$\frac{dN_{gas,i}}{dt} = -N_{tot} \cdot \frac{dN_{p,i}}{dt} - N_{gas,i} \cdot \mathrm{WLC} \quad \text{(S2)}$$

where $N_{p,i}$ and $N_{gas,i}$ are the number of molecules *i* in a particle and in the gas phase, d_i and d_p are the diameters of molecule *i* and the particle, $D_{air,i}$ and $D_{air,p}$ are the gas phase diffusion coefficients of vapor molecule *i* and a particle, β_i is the transition regime correction factor for mass transport for vapor i and it's calculated based on the version by *Lehtinen and Kulmala*, [2003], k_B is the Boltzmann constant, T is the temperature, $p_{\infty,i}$ and $p_{eq,i}$ are the partial vapor pressure of *i* in the gas phase and the equilibrium vapor pressure of *i* at the particle surface, N_{tot} is the number concentration of particles and WLC is the vapor wall loss coefficient.

The model assumes ideal solution and the equilibrium concentration for compound *i* is thus $p_{eq,i} = X_i \cdot p_{sat,i} \cdot \mathrm{Ke}$, where X_i is the molar fraction in the particle phase, $p_{sat,i}$ is the saturation vapor pressure and Ke is the Kelvin factor of *i*. In terms of the saturation concentration (C_i^*) the equilibrium concentration can be written as

$$p_{eq,i} = X_i C_i^* \frac{RT}{M_i} \exp\left(\frac{4\sigma v_i}{RTd_p}\right) \cdot 10^{-9} \quad \text{(S3)}$$

where R is the gas constant, M_i and v_i are the molar mass and molar volume of i and σ is the surface tension of the particle. The exponential term in Eq. (S3) is the Kelvin factor. Eq. (S3) gives $p_{eq,i}$ in pascals when C_i^* is given in μg m^{-3} (thus the factor 10^{-9}) and other variables in SI units.

The vapor wall loss coefficients (WLC) for the organic vapors in the evaporation chamber are not known. The effect of vapor wall losses was tested by carrying out the evaporation experiments in dry conditions with two different particle number concentrations differing approximately by one order of magnitude. The measured evaporation rates in these two cases did not differ much. Based on model simulations, such a similarity in the evaporation rates despite the difference in particle concentrations suggest that the vapor wall losses were fast with approximately WLC ≥ 10^{-2} s^{-1} (Fig. S2). Therefore, in the model simulations we assumed that all of the evaporated vapors were lost on walls immediately (infinite WLC) unless otherwise stated.

Only organic compounds were included in the model system when simulating the particle evaporation in the dry conditions. For simulating the evaporation in humid conditions water was included in the model system. The amount of water in a particle was calculated assuming constant equilibrium between gas and particle phase and two different methods were used:

Method 1 (basic version of the model): The number of water molecules in a particle was calculated at each time step based on the criteria

$$p_{eq,water} = \frac{\mathrm{RH}}{100\,\%} \cdot p_{sat,water} \quad \text{(S4)}$$

where $p_{eq,water}$ is the equilibrium vapor pressure of water above the particle surface and $p_{sat,water}$ is the saturation vapor pressure of pure water. Here the ideal solution assumption was used also for water (unity activity coefficient) and the Kelvin effect was taken into account.

Method 2: Number of water molecules in a particle was calculated based on measured hygroscopic growth factors (HGF) of α-pinene SOA particles. The hygroscopic growth factor is defined as the ratio between the dry ($d_{p,dry}$) and wet ($d_{p,wet}$) particle diameters (HGF = $d_{p,wet}/d_{p,dry}$). We assumed that the molecular volumes (v) in a mixture equal those of pure compounds in which case the number of water molecules in a particle is

$$N_{p,water} = \left(\mathrm{HGF}^3 - 1\right) \frac{\sum_i N_{p,i} v_i}{v_{water}} \quad \text{(S5)}$$

where the summation goes over the organic compounds. The HGF was assumed to be size independent, i.e. HGF value stayed the same along the evaporation.

2.2 Multi-layer particle evaporation model

The multi-layer particle evaporation model is based on the Kinetic multi-layer model for gas-particle interactions in aerosols and clouds (KM-GAP) [*Shiraiwa et al.*, 2012; *Shiraiwa et al.*, 2013]. In KM-GAP the gas-particle system is divided into multiple layers: gas phase, near-

surface gas, sorption layer at the particle surface, particle surface layer and multiple particle bulk layers. KM-GAP simulates particle evaporation/condensation based on molecular fluxes in and between gas, particle surface and particle bulk. The model was modified regarding the treatment of the surface layer. In the modified version a new surface layer (ss layer in Shiraiwa et al. [2013]) is formed by combining the surface layer with the first particle bulk layer when the thickness of the surface layer reduces to less than a prescribed value. In our simulations this value was 0.5 nm. As a result, the number of layers is decreasing along the particle evaporation. This modification allowed for simulating the evaporation of particles where there is no non-volatile compound (e.g. seed particle). The particle bulk was initially divided into 30 layers. Effect of the number of particle bulk layers was tested and for ≥ 30 layers the model results were stable with respect to the change in number of layers.

The multi-layer model was applied for dry and 40% RH experiments. For the 40% RH experiment water was included in the model by assuming ideal solution and constant instantaneous equilibration between gas phase and particle surface for water. Transport of water molecules between surface and particle bulk phase and within particle bulk was calculated similarly as for the organic compounds. Organics were treated as an ideal solution (i.e. activity coefficients were unity), desorption lifetimes of all organic compounds were assumed to be 10^{-6} s and other properties were the same as in the well-mixed particle evaporation model.

2.3 Fitting of VBS using the genetic algorithm

The well-mixed particle evaporation model calculates the particle diameter as a function of time based on the initial particle phase mass fractions and the properties of each compound provided as inputs. We presented the multi-component SOA particles using an 8-bin volatility basis set (VBS). In order to find a satisfactory set of eight initial mass fractions that produce an evaporation similar to the observations, the parameter space was explored heuristically using the genetic algorithm (GA) [*Goldberg*, 1989], which mimics natural selection.

Ultimately, the goal of the GA in this work is to minimize the fitness function

$$F\left(y_i ; y_{m,i}\right) = \sum_{i=1}^{n} \left[y_i\left(t_i\right) - y_{m,i}\left(t_i\right)\right]^2 \qquad \text{(S6)}$$

where y_i and $y_{m,i}$ are the measured and modelled particle size normalized by the initial size $d_p/d_{p,o}$ at time t_i, respectively. The summation in equation (S6) is over the measured data points. The working principle of the GA in this study can be broken down into 5 steps:

1) Create the first generation of initial mass fractions.
2) Perform evaporation simulation for each member of the generation.
3) Calculate the fitness of each member in the first generation.
4) Create the next generation.
    a. Select two parents.
    b. Create a child from the parents.
    c. Perform mutation to the child.
    d. Perform evaporation simulation to the child.
    e. Calculate the fitness of the child.
    f. If the fitness of the child is better than the worst individual in the previous generation accept the child to the new generation. Otherwise accept one of the parents.

g. Go to (a) if the size of the new generation is smaller than the previous generation.

5) Repeat step 4 until the absolute difference between the fitnesses of the best members of the current and previous generation is smaller than $\varepsilon = 10^{-5}$ or until a predetermined amount of generations has been created.

In our simulations, each member of a generation consists of eight mass fractions which represent the relative amount of the eight C^* bins (10^{-3}-10^{4} μg m^{-3}) in a particle at the beginning of the evaporation. In the first generation the mass fractions of each member are created randomly. For the creation of pseudorandom numbers, we used the Mersenne twister algorithm.

The most complicated parts of the GA are steps 4a and 4b. Choosing parents from an entire population is not a straightforward task. If only the best members are constantly chosen as parents the parameter space might not be explored thoroughly. If the members are chosen to be parents with equal probability the algorithm might not converge to a minimum of the fitness function. In this study, we used the exponential function to calculate the probability of each member to be chosen as a parent

$$P(\text{parent}) \propto \exp\left(\frac{F_m}{T}\right) \tag{S7}$$

where F_m is the value of the fitness function (S6) of that particular member and T is determined as the difference between the worst and best fitness of the members of the previous generation. This way when T is large, members with larger values of the fitness function have higher probability to be chosen as parents compared with the situation where T is small. Equation (S7) also ensures that the better members are chosen as parents more often than the worse members.

After the parents are selected the mass fractions of the child are calculated from the parents' mass fractions as

$$X_{mass,i,child} = X_{mass,i,l} + \frac{F_l}{F_h}\left(X_{mass,i,l} - X_{mass,i,h}\right) \tag{S8}$$

where $X_{mass,i}$ is the mass fraction of VBS bin i and subscripts l and h refer to the parents which have lower and higher value of the fitness function, respectively. Using equation (S8) means that one compares the parents' mass fractions and assumes that, if parent 1 has smaller value of the fitness function than parent 2 it is due to the fact that the mass fractions differ between the parents by some amounts $\Delta X_{mass,1}$ ... $\Delta X_{mass,8}$. The algorithm then tries to change each mass fraction of the child in the same direction where the difference between the parents points. In order to not take too large steps in one generation this change is scaled by the factor proportional to the values of the fitness functions of the parents.

The use of equation (S8) ensures that the sum of child's mass fractions equal unity but allows negative mass fractions to occur. That is why every child is checked for negative values of the mass fractions and, in the event of finding those, the mass fraction with the negative value is changed to zero and an amount equal to the negative value is removed from the next, less volatile bin(s).

Finally, a mutation is performed on the child by randomly changing two mass fractions with each other with probability $p_{mutation}$ = 5%. The child is accepted to the new generation if the

value of the fitness function is lower than the worst value in the previous generation. If the fitness function has higher value, one of the parents is selected to the next generation with equal probability.

In addition, in step 4 the child is not accepted to the new generation if the volatility distribution suggests unreasonably high oxidized organic concentration compared to the reacted α-pinene (200 ppb). The limit is set as

$$\sum_i \left(X_i C_i^* \right) < C_{reacted} \quad \text{(S9)}$$

where X_i is the dry particle molar fraction of compound *i* and $C_{reacted}$ is the mass concentration of the reacted α-pinene. The left hand side of eq. (S9) describes the gas phase concentration of the condensing organics at the end of the flow tube assuming that gas-particle equilibrium is reached. In the cases where the oxidized organic mass concentration suggested by the volatility distribution is higher than the allowed, new parents are chosen and a new child calculated until this mass balance criterion is met. The mass balance criterion is approximate as it doesn't take into account the increase in organic mass with oxidation (addition of O), vapor wall losses or particle phase organic mass (< 10% of reacted α-pinene mass). These factors are expected to cause negligible effect on the results as applying the mass balance criterion described in eq. (S9) caused only a minor effect on the results compared to applying no such mass balance limit.

We performed 20 set of genetic algorithm simulations, each with 15 generations and 200 members per generation, for the dry, 40% and 80% RH experiment. The model simulation with the smallest fitness value from each simulation set was selected giving 20 different initial compositions. The best fit initial composition was chosen from these 20 cases as the one with the smallest fitness function value. Out of the 20 cases we considered only those with fitness < 0.002 (16 for dry, 20for 40% RH, 20 for 80% RH) when reporting the variability in the initial composition (Fig. 1 A, 2 A-B).

2.4 Effect of theoretical treatment of water uptake

The basic version of the well-mixed particle evaporation model calculated water content of a particle assuming an ideal solution. The initial particle composition optimized for 80% RH with this basic version is shown in Fig. 1 B. When modelling the evaporation at 40% RH we tested how the theoretical treatment of particle water uptake affected the model predictions. This was done by using the experimentally determined hygroscopic growth factors (HGF) of α-pinene SOA to calculate water uptake. The best fit initial VBS determined at 80% RH using HGF = 0.05 [*Pajunoja et al.*, 2015; *Varutbangul et al.*, 2006] and the corresponding size evolution are shown in Fig. S3 A-B. This initial VBS was used for simulating the evaporation with the well-mixed particle evaporation model at 40% RH using HGF = 0.01 [*Varutbangul et al.*, 2006]. Results for RH40% are shown in Fig. 2B and also in Fig. S3 (blue dashed line). The best fit initial VBS and the variability within the genetic algorithm simulations in the HGF simulations at 80% RH show a similar general pattern as compared to the ideal solution simulations. Also with HGF representation of water uptake, 20 genetic algorithm simulation sets were performed (all 20 resulting initial compositions had fitness < 0.002).

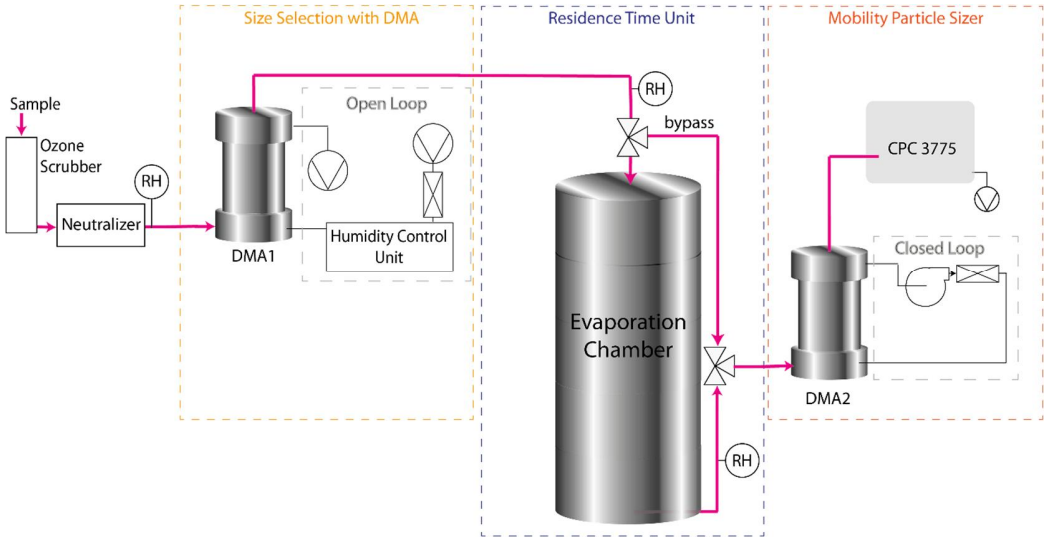

Figure S1. Schematics of particle size measurement system. Pink line represents sample line from polydisperse sample to the evaporated monodisperse sample. The SMPS system on the right hand side was TSI model 3080 and both high and low flow modes were used depending on the target residence time. The humidity control unit in the DMA sheat line was optional and only in use in 40% and 80% RH experiments.

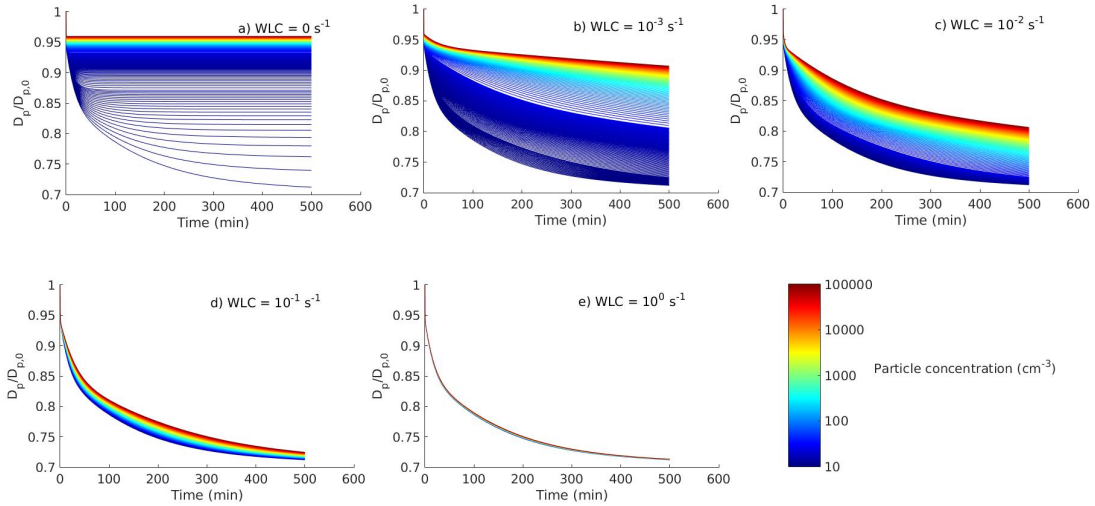

356

357 **Figure S2.** Time evolution of particle diameter normalized with the initial diameter (80 nm) at
358 dry conditions. Circles: measured size evolution. Lines: Size evolution simulated with the well-
359 mixed particle evaporation model with different assumptions of the vapor wall loss coefficient
360 (WLC) and for different particle concentrations (indicated with the line color). The initial particle
361 composition was the same in all simulations.

362

363

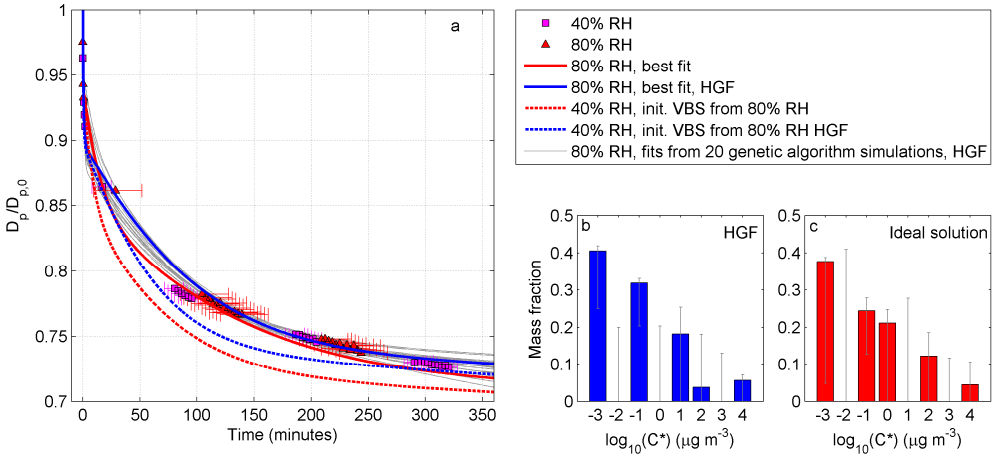

Figure S3. Measured evaporation of particles with initial size 80 nm and model simulations at 40% and 80% RH with different treatment of particle water uptake. Time evolution of particle diameter normalized with the initial diameter (a). Squares and triangles show measured evaporation at 40% and 80% RH, respectively. The error bars in time originate from the chamber filling time. Well-mixed particle model simulations at 40% and 80% RH with water uptake calculated based on ideal solution assumption: Simulation with the best fit initial volatility distribution at 80% RH (red solid line) and simulation with the corresponding initial composition (shown in c) at 40% RH (red dashed line). Well-mixed particle model simulations at 40% and 80% RH with water uptake calculated based on HGF: Simulation with the best fit initial volatility distribution at 80% RH (blue solid line) and simulation with the corresponding initial composition (shown in b) at 40% RH (blue dashed line). Error bars in b-c show the variability in the initial volatility distributions (minimum and maximum) within the best fits from 20 genetic algorithm simulations. The corresponding size evolutions for HGF case at 80% RH are shown in a (gray lines). The corresponding size evolutions for ideal solution case are shown in Fig. 1 a.

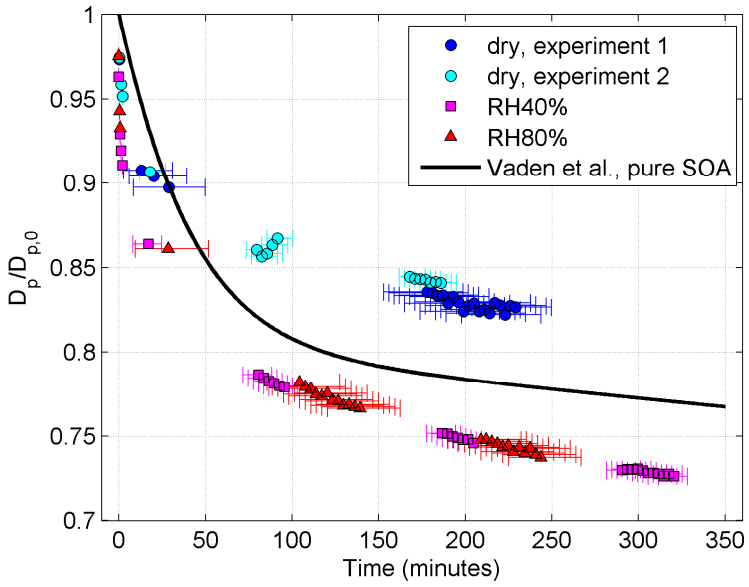

Figure S4. Time evolution of particle diameter normalized with the initial diameter (80 nm) measured in this study under dry (circles), 40% RH (squares) and 80% RH (triangles) conditions. The error bars in time originate from the chamber filling time. Black line shows the biexponential fit by Vaden et al. [2011] on their measured evaporation of particles (initially 125-251 in diameter) under dry conditions.

389 **Movie S1.** Modelled evolution of particle size and composition at 80% RH. Time evolution of
390 particle diameter normalized with the initial diameter: triangles show measured evaporation
391 with error bars in time originating from the chamber filling time and line shows the well-mixed
392 particle evaporation model simulation with the best fit initial particle composition. The
393 corresponding particle composition development is shown in the inset.
394
395